Available online at www.sciencedirect.com
ScienceDirect
Journal of the European Ceramic Society 27 (2007) 2127–2135
www.elsevier.com/locate/jeurceramsoc

Electrochemical corrosion of solid and liquid phase sintered silicon carbide in acidic and alkaline environments

A. Andrews [a], M. Herrmann [b,*], M. Sephton [a], Chr. Machio [a], A. Michaelis [b]

[a] *School of Chemical & Metallurgical Engineering, University of the Witwatersrand, P/Bag 3, Wits 2050, Johannesburg, South Africa*
[b] *Fraunhofer Institute for Ceramic Technologies and Systems, Winterbergstrasse 28, Dresden D-01277, Germany*

Received 20 March 2006; received in revised form 26 June 2006; accepted 7 July 2006
Available online 25 September 2006

Abstract

Solid and liquid phase sintered silicon carbide (SiC) ceramics are used in aggressive environments, e.g. as seals and linings in chemical plant equipments. There exist data concerning corrosion of solid phase sintered SiC (SSiC), but there are only few data concerning their electrochemical corrosion behaviour. The corrosion of liquid phase sintered SiC ceramics (LPS SiC) containing yttria aluminium oxide grain boundary phases has been investigated by standard methods that have shown the decisive influence of the oxide grain boundary on the corrosion stability of these materials. But no electrochemical investigations are known. In this study therefore, potentiodynamic polarisation measurements have been used to determine the corrosion mechanisms of SSiC and LPS SiC ceramics at room temperature in acidic and alkaline environments. The investigation has shown a pronounced electrochemical corrosion in acids and alkaline solutions for both types of materials. In HCl and HNO_3 pseudo-passivity features due to the formation of a thin layer of SiO_2 on the surface were observed, whereas in NaOH soluble silicate ions were observed resulting in more pronounced corrosion. Microstructural observations of initial and corroded samples revealed that the residual carbon found in the microstructure of SSiC did not dissolve preferentially. The corrosion current densities of the LPS SiC materials were caused by the dissolution of SiC and not by the corrosion of the oxide grain boundary phase. The corrosion current densities of the LPS SiC materials investigated were lower than those of the SSiC materials.

Keywords: LPS SiC; Corrosion; SiC; Electrochemical corrosion

1. Introduction

Ceramic materials are often used in very aggressive and corrosive environments, e.g. bearings, seals, valves, and linings in chemical equipment because of their high degree of chemical inertness and corrosion resistance. However, even though it is slow, corrosion does occur. The standard procedure for measuring corrosion resistance of ceramic materials is the immersion method that involves immersing samples in a corrosive medium and measuring weight loss, corrosion layer depth, residual strength and sometimes the concentration of the corroded ions in the corrosion media.[1–7] Electrochemical methods are often used to determine corrosion behaviour of metals and hard metals, but are hardly ever used for the analysis of ceramic materials. However, these techniques can also be used to measure the corrosion behaviour of ceramics as long as the ceramics remain electrically conducting.[2] These methods offer the possibility to further elucidate corrosion mechanisms and stability of conducting or partially conducting ceramic materials, thus enhancing the understanding of ceramic material corrosion behaviour. Recent investigations have shown that the corrosion of SiC can be strongly influenced by electrochemical effects.[7]

The electrochemical corrosion behaviour of a material can be described using the open circuit potential (potential formed at the interface of a material and a solution if no external voltage is applied and no macroscopic current flows), the corrosion current density (i_{corr}), or the current at different applied voltages. These values are normally determined using polarisation scans[8] during which the potential at the interface of a test surface is continuously changed and the current passing monitored. The open circuit potential is a measure of the ease with which the material dissolves in a solution in which it is immersed, i.e. the ease with which the surface corrodes. The potential is directly proportional to the energy changes accompanying corrosion. The

* Corresponding author.
E-mail address: herrmann@ikts.fhg.de (M. Herrmann).

0955-2219/$ – see front matter © 2006 Published by Elsevier Ltd.
doi:10.1016/j.jeurceramsoc.2006.07.011

corrosion current density (i_{corr}) is directly proportional to the corrosion rate of the material if no external voltage is applied.

Electrochemical corrosion of sintered silicon carbide ceramics has been studied at room temperature in various dilute acids (HCl, HNO_3, HF, H_2SO_4 and H_3PO_4).[2,5] The principal corrosion reaction of SiC was assumed to be the dissolution of Si atoms. This is valid in the case where the SiC is infiltrated with Si, i.e. for the case of SiSiC but not for SSiC where the corrosion is connected with the SiC. There were no measurements in alkaline environments in these investigations.[2,5]

Investigations by Cook et al.[2] deduced the thermodynamic requirements, in terms of the open circuit potentials, for SiC corrosion based on Si reactions. From the different behaviour in HF and HCl, they deduced that SSiC was passive, i.e. did not corrode in acidic environments, except in HF, because of the formation of a surface film of silica. The surface film acted as a barrier between the SSiC and the corrosive medium. The reduction of O_2 dissolved in water was proposed as the cathodic reaction. A number of anodic reactions for carbon and silicon in acidic and alkaline environments, with their corresponding standard potentials (E^0), are available in literature.[9–11] Based on these reactions and using the thermodynamic data[12] of reaction (1) below:

$$Si + C \leftrightarrow SiC \quad (1)$$

the following corrosion reactions for SiC were proposed and their standard potentials (i.e. tendencies to corrosion) (versus standard hydrogen electrode, SHE) were calculated as shown in Eqs. (2)–(9).

In acidic environments:

$$C(\text{residual}) + 2H_2O(l) \rightarrow CO_2(g) + 4H^+(aq) + 4e^- \quad E^0 = +0.206\,V \quad (2)$$

$$SiC(s) + 2H_2O(l) \rightarrow SiO_2(s) + C + 4H^+(aq) + 4e^- \quad E^0 = -1.07\,V \quad (3)$$

$$SiC(s) + 4H_2O(l) \rightarrow SiO_2(s) + 8H^+(aq) + CO_2(g) + 8e^- \quad E^0 = -0.433\,V \quad (4)$$

$$SiC(s) + 3H_2O(l) \rightarrow SiO_2(s) + 6H^+(aq) + CO(g) + 6e^- \quad E^0 = -0.542\,V \quad (5)$$

In alkaline environments:

$$C(\text{residual}) + 6OH^-(aq) \rightarrow CO_3^{2-}(aq) + 3H_2O(l) + 4e^- \quad E^0 = +1.72\,V \quad (6)$$

$$SiC(s) + 6OH^-(aq) \rightarrow SiO_3^{2-}(aq) + C + 3H_2O(l) + 4e^- \quad E^0 = -1.87\,V \quad (7)$$

$$SiC(s) + 12OH^-(aq) \rightarrow SiO_3^{2-}(aq) + 5H_2O(l) + CO_3^{2-}(aq) + 8e^- \quad E^0 = -0.076\,V \quad (8)$$

$$SiC(s) + 8OH^-(aq) \rightarrow SiO_3^{2-}(aq) + 4H_2O(l) + CO(g) + 6e^- \quad E^0 = -0.80\,V \quad (9)$$

The oxide additives (yttria and alumina (Y_2O_3/Al_2O_3)) in LPS SiC materials form crystalline phases at the SiC grain boundaries. Some Al, O and Y can dissolve in the SiC grains and can strongly influence the electrical behaviour[13–15] of the resulting material. LPS SiC materials show in comparison to SSiC materials, increased fracture toughness and flexural strength, but also different corrosion resistance and high temperature properties.[1,3,4,15,16] It is therefore essential to know the effect of the oxide grain boundary phases which result from the oxide additives on the corrosion resistance of these materials. The proposed electrochemical reactions ((2)–(9)) of the SiC grains in SSiC are similar to those which could be expected in LPS SiC but the presence of an oxide grain boundary phase and the dissolved Al, O and Y ions in the SiC grains in the LPS SiC material could influence the mechanism of corrosion. The oxide grain boundary phases in the LPS SiC materials are mostly different yttria aluminates ($Y_3Al_5O_{12}$, $YAlO_3$, $Y_4Al_2O_9$). They could undergo severe dissolution in acidic environments. For example yttria aluminium garnet ($Y_3Al_5O_{12}$) can dissolve according to the following reaction:

$$Y_3Al_5O_{12} + 24H^+(aq) \leftrightarrow 3Y^{3+}(aq) + 5Al^{3+}(aq) + 12H_2O(l) \quad (10)$$

Reaction (10) above is a simple hydrolysis reaction without an exchange of electrons and therefore cannot result in an electrical current. In strong alkaline environments, aluminium and yttrium react to form soluble $[Al(OH)_6]^{3-}$ or AlO_2^- ions and insoluble yttrium hydroxide, respectively.

In this paper, the corrosion mechanisms of SSiC and LPS SiC in acidic and alkaline environments are investigated by electrochemical methods. Microstructural observations before and after corrosion as well as the concentration of corroded ions in solution were analysed and correlated with the corrosion mechanism.

2. Experimental procedure

2.1. Materials

Two liquid phase sintered SiC ceramics (LPS SiC) with different additive ratios of Y_2O_3/Al_2O_3 (1:1 and 1:4, respectively) and a solid state sintered silicon carbide (SSiC) material were used. The LPS SiC materials were sintered at a temperature of 1950 °C for 60 min. The materials' characteristics are shown in Table 1. Details of the preparation are given in Ref.[15].

The SSiC ceramic materials were sintered with carbon and boron as sintering additives. The weight percent of the resid-

Table 1
Material compositions of LPSSiC- and SSiC-materials

Material	SSiC	LPSSiC-1	LPSSiC-2
Additives	B/C	Y_2O_3/Al_2O_3 (10 wt%)	Y_2O_3/Al_2O_3 (10 wt%)
Mol ratio additives Y_2O_3/Al_2O_3		1:1	1:4
Measured density (g/cm^3)	3.11	3.32	3.26
Theoretical density (g/cm^3)		3.36	3.34
Grain boundary phase	2% carbon	$Y_3Al_5O_{12}$, $Y_4Al_2O_9$	$Y_3Al_5O_{12}$, Al_2O_3
Resistivity (kΩ cm)	39.5	61	39

ual carbon, determined using an X-ray diffraction technique (Rietveld analysis) was $2 \pm 0.4\%$. The measured density was 3.11 g/cm^3. The specific resistivity of the LPS SiC materials was in the range of 40–60 kΩ cm, the resistivity of the SSiC material was 39 kΩ cm (Table 1).

Samples were prepared for image analysis and corrosion experiments by grinding on Struers MD-Piano 1200 to achieve a flat surface and polishing on a Pan cloth to 1 μm finish using diamond spray and diamond extender (lubricant). The samples were cleaned afterwards with ethanol and dried. The microstructures and compositions of the material before and after corrosion were analysed using a LEO1525 scanning electron microscope. X-ray diffraction (PW 1710 Phillips; XRD7, GE) was used to determine the composition of the materials and it was found that the major oxide phase was $Y_3Al_5O_{12}$, i.e. yttria aluminium garnet, YAG (Table 1).

2.2. Corrosion measurements

Potentiodynamic polarisation measurements were performed according to ASTM G 5-94[17] and ASTM G 3-89[18] to investigate the corrosion behaviour of the test samples. Samples were prepared by attaching an insulated copper wire using a conducting paste to one face of the sample and cold mounting in resin. Samples were then polished on a Pan cloth to 1 μm surface finish and coated at the sample-resin interface with Bostik quickset to prevent the possibility of crevice corrosion. The area of the surface exposed to the corrosive media was 0.1 cm^2 for SSiC and 1 cm^2 for LPS SiC materials. This was followed by cleaning in an ultrasonic bath with ethanol before immersion in the corrosive medium (electrolyte). All tests were conducted at room temperature (25 °C). A schematic diagram of the experimental setup is shown in Fig. 1a. The potentiostat automatically varies the potential at the exposed surfaces at a constant rate, which potential generates current through the cell (Fig. 1a). The current goes through the working electrode (sample) and the counter electrode (CE). The counter electrode used was platinum. The potential of the working electrode was measured with respect to the reference electrode (REF) connected via a salt bridge and the Luggin capillary. The reference electrode used was a saturated calomel electrode (SCE) (potential of the standard hydrogen electrode SHE = SCE + 241 mV). The capillary was suspended approximately 1 cm above the sample surface. A typical polarisation measurement curve obtained from such experiment is shown in Fig. 1b. Information that could be obtained from such graphs include open circuit potential (E_{corr}), corrosion current density (i_{corr}) and Tafel slopes. i_{corr}, which is directly proportional to the corrosion rate, is determined by Tafel extrapolation method in which the linear regions of the potential versus current curve are extended until they meet as indicated in Fig. 1b.[18]

The open-circuit potential (E_{corr}) was taken 5 min after immersion of samples. A potentiodynamic scan was then carried out with a scan rate of 1 mV/s. The width of the scan was from −200 mV to about +1000 mV relative to E_{corr}. At least three full scans were conducted per electrolyte. Samples were re-polished and used in subsequent scans. The electrolytes

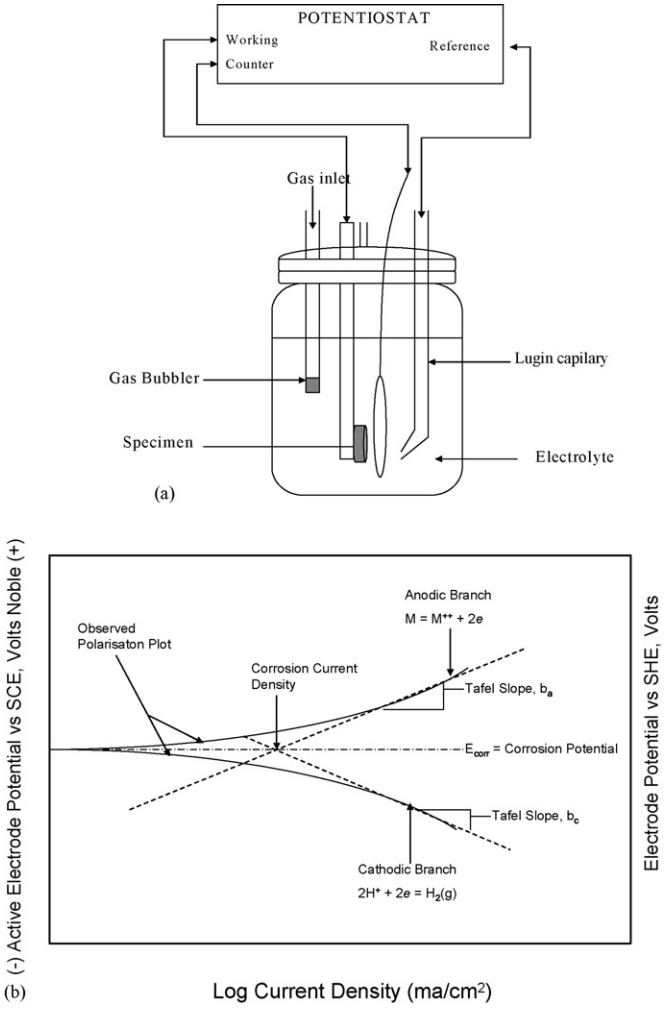

Fig. 1. (a) Schematic diagram of the setup used for the potentiodynamic polarisation tests and (b) typical Tafel plot from polarisation experiment (ASTM G3-89).

used in this investigation included 1 M solutions of HCl, HNO_3 and NaOH. The electrolytes were replaced after each polarisation scan. Before immersion of the samples, the electrolytes were purged with ultra-high purity (99.999%) nitrogen gas for approximately 45 min to reduce the dissolved-oxygen content. Purging was continued throughout the tests. In experiments aimed at determining corrosion mechanisms, the SSiC material was tested in HCl purged with CO_2 gas while the LPS SiC was tested in an electrolyte made from 50 g/l yttrium chloride (YCl_3) in 1 l of 1 M HCl. Also, the electrolyte was analysed after polarisation scans using inductively coupled plasma optical emission spectrometry (SPECTRO CIRUS CCD). The following analytical wavelengths were chosen (nm): 396.156 Al, 251.611 Si, and 371.030 Y. These wavelengths showed a good linear response between concentration and intensity and were free from interferences in the range of concentrations used in the present study.

3. Results

3.1. Corrosion behaviour of SSiC ceramic

Table 2 shows a summary of the corrosion current densities and corrosion potentials measured for all materials in the different corrosive environments. Fig. 2 shows typical polarisation scans of SSiC in HCl (Fig. 2a and c), NaOH (Fig. 2b) and in HNO_3 (Fig. 2d). The reproducibility of the potentiodynamic behaviour was good (Fig. 2a and b). In both acids (HCl, HNO_3) different open circuit potentials were observed indicating the influence of the acidic anion on the corrosion (Table 1, Fig. 2). The corrosion potential and the corrosion current in HCl did not change with the gas used to purge the electrolyte, i.e. (CO_2 or N_2; Fig. 2c).

To evaluate the possible formation of passivating layers during the potentiodynamic polarization of SSiC, a test specimen, i.e. the working electrode was held at a potential more positive value than the corrosion potential (+500 mV versus SCE) in 1 M HNO_3 for 30 min. This resulted in the shift of the open circuit potential to positive potentials (Fig. 2d). This sample was then immersed in 1 M HF for 10 min (without applying potential) followed immediately by potentiodynamic polarization in 1 M HNO_3. The polarisation scan of this sample after immersion was nearly identical with the one observed for the as-prepared samples (Fig. 2d). This indicated that the oxide layer formed was dissolved by the HF, indicating the layer formed was $SiO_2{\cdot}H_2O$ because HF dissolves SiO_2.

The open circuit potential in 1 M NaOH was much more positive than that in HCl (Fig. 2b) and was similar to that in HNO_3. The SEM image of the SSiC material before and after corrosion is shown in Fig. 3. The images show that carbon (black inclusions in the image) was not attacked, but that there was a slight increase in the porosity. The corrosion of the SSiC in the different media is described in detail in Ref.[19]

3.2. Corrosion behaviour of LPS SiC ceramics

Typical polarisation scans of LPS SiC-1 and LPS SiC-2 materials in 1 M HNO_3 and in 1 M NaOH are shown in Fig. 4. Similar behaviour was obtained in 1 M HCl (Table 2). The reproducibility of the open circuit potential, E_{corr}, was not good. However, the corrosion current densities, i_{corr}, were reproducible. Samples were re-polished between the different scans, so that for every scan a fresh surface was used. The corresponding SEM micrographs before and after corrosion are shown in Fig. 5.

Additional corrosion tests of LPS SiC-1 were performed by immersing a sample in 1 M HCl and holding at a potential more positive than the corrosion potential (+300 mV versus SCE) for 30 min. Another sample was immersed in 1 M HCl for 30 min without applying a potential and the SEM micrographs were used to determine the effect of these treatments (Fig. 5). It appears that there were no significant differences after 30 min of

Table 2
Summary of corrosion current densities and corrosion potentials at different conditions

Materials	Condition (s)	Corrosion potential (mV vs. SCE)	Corrosion potential (mV vs. SHE)	Current density, i_{corr} ($\mu A/cm^2$)
SSiC[a]	1 M HCl	?	?	7
SSiC	1 M HCl	−124 (−124; −119; −130)[b]	+115	46 (55; 50; 35)[b]
	1 M HNO_3	+78 (+76; +81; +79)[b]	+319	58 (55; 55; 65)[b]
	1 M HNO_3 (60 min hold)	+147	+38	0.04
	1 M HNO_3 + 1 M HF	+78	+319	40
	1 M NaOH	+53	+294	33
	1 M NaOH (30 min hold)	+73	+314	35
	1 M NaOH	+50.81 (41.48; 54.48; 56.47)[b]	+291.81	33 (30; 30; 40)[b]
Si	1 M HCl	−380	−139	1
	1 M NaOH	−846	−605	0.9
LPSSiC-1	1 M HCl	−215 (−216; 215; −215)[b]	+26	2 (1.8; 1.8; 2)[b]
	1 M HNO_3	−87 (−145; −95; −21)[b]	+154	6 (4; 4; 10)[b]
	1 M NaOH	−260 (−292; −253; −236)[b]	−19	1.8 (2; 1.5; 2)[b]
LPSSiC-2	1 M HCl	−304 (−377; −312; −222)[b]	−63	0.07 (0.07; 0.08; 0.05)[b]
	1 M HNO_3	−32 (−185; −38; +128)[b]	+206	0.09 (0.08; 0.075; 0.1)[b]
	1 M NaOH	−421 (−544; −408; −310)[b]	−180	0.06 (0.09; 0.045; 0.04)[b]

[a] Data from Cook et al.[2]
[b] In parenthesis are the different measured values.

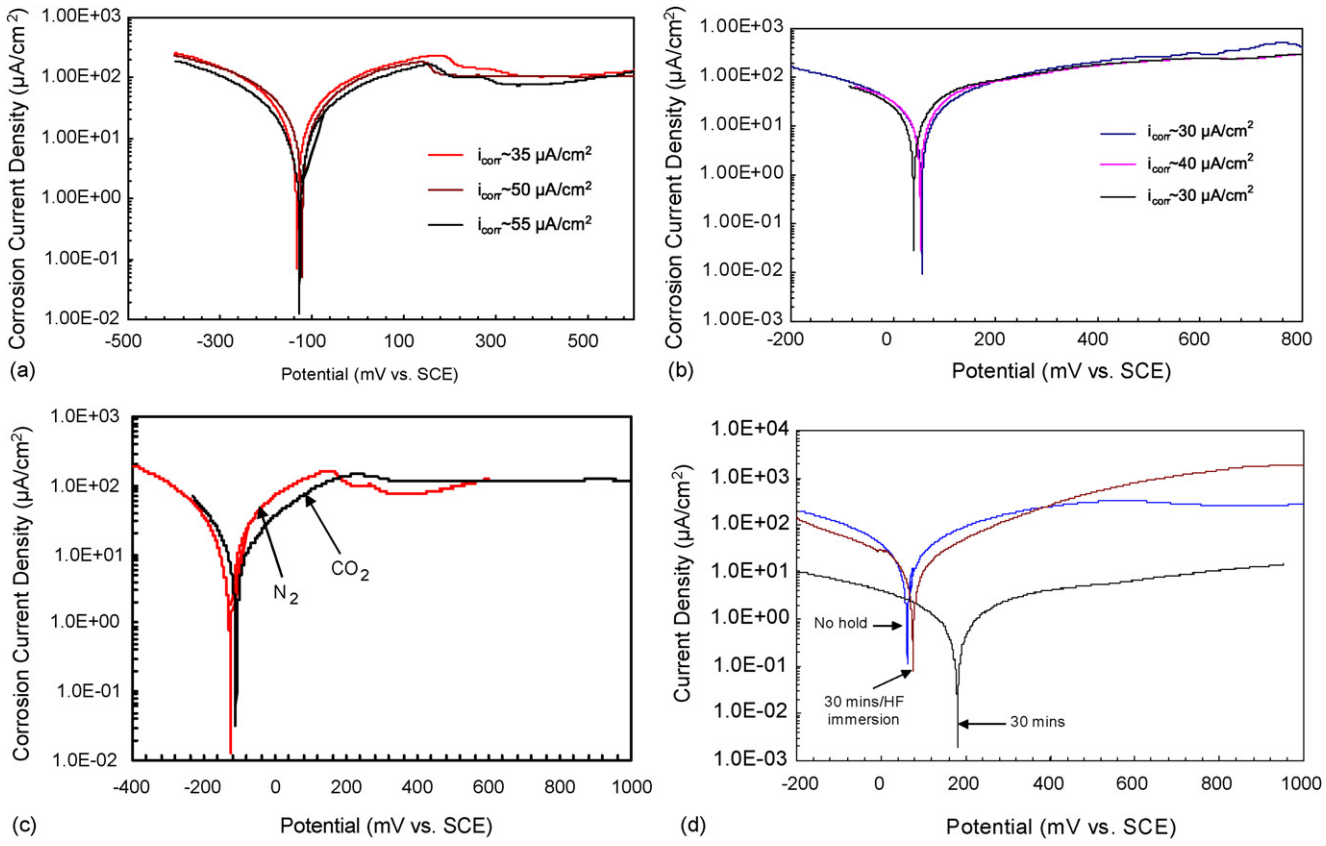

Fig. 2. Polarisation scans of SSiC in different solutions. (a) 1 M HCl, (b) 1 M NaOH, (c) 1 M HCl when de-aerated with N_2 and CO_2 gas (approximately the same i_{corr} and E_{corr}) and (d) sample was held at +500 mV for 0, 30 min in 1 M HNO_3 followed by 10 min immersion in 1 M HF before performing a full scan.

immersion and immersion plus holding at +300 mV in 1 M HCl. In both cases, the dissolution of the grain boundary regions was much more pronounced than the dissolution of the SiC grains. This is in agreement with the observed concentration of Al, Y and Si in the solution after the polarisation scan (Fig. 6).

The polarisation scans of LPS SiC-1 in NaOH are shown in Fig. 4c. The reproducibility of the E_{corr} of both the LPS SiC materials in NaOH was not good. The average corrosion current densities and average corrosion potentials are shown in Table 2. The surfaces were not as severely damaged as in the acidic environments (Fig. 5).

4. Discussion

The polarisation plots of the investigated SSiC- and LPS SiC-materials are similar, but there is a systematic shift of the open circuit potential to more negative values for the LPS SiC materials in comparison to the SSiC material (Table 2). This implies that the tendency to corrode was higher for the LPS SiC than the SSiC materials because the lower the E_{corr}, the earlier the material will start corroding in a particular environment and vice versa. However, the rate of corrosion is determined by the corrosion current density.[8] The corrosion current densities of the SSiC materials were more than 10 times higher than the values observed for the LPS SSiC materials. This implies that the SSiC materials corroded faster than the LPS SiC materials. Material LPS SiC 2 had a corrosion current density that was an order of magnitude lower than for the LPS-SiC 1 material under the same conditions. These conclusions are valid despite the large scatter in the E_{corr} values of the LPS SiC materials. With these differences in mind, we will discuss first the electrochemical reactions of the SiC grains. The corrosion current density of SSiC in HNO_3 strongly reduced with time and the open circuit potential shifted to values that are more positive. By adding HF to the HNO_3 acid or by treatment of the samples with HF after a polarisation scan, this drop of the corrosion current could be avoided. Also in NaOH such drop of corrosion has not been observed.[19] These results confirm the proposal by Cook et al. about the formation of a passivating SiO_2 surface layer. The formation of a protecting SiO_2 layer on the surface is also proved by the much lower Si-concentration in the solution observed after corrosion in HCl in comparison to the corrosion in NaOH (Table 3) (the current densities in both cases were similar Table 2).

A comparison of the microstructures of the SSiC materials before and after corrosion revealed that the corrosion attack was not homogeneous but mostly took place at the inter-

Table 3
Concentration of dissolved silicon after holding at +500 mV prior to polarisation scan

Sample	Si concentration (ppm)
30 min hold prior scanning in 1 M HNO_3	0.37
30 min hold prior scanning in 1 M NaOH	20.9

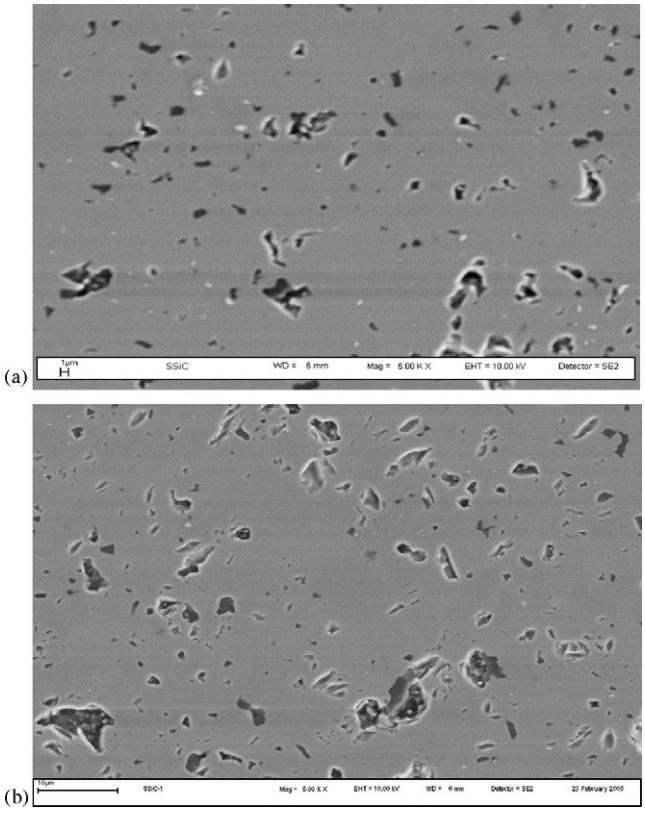

Fig. 3. SEM (secondary) micrograph of SSiC. (a) Before corrosion and (b) after full polarisation scan in 1 M HNO_3. Sample was held at +500 mV for 60 min.

faces. The micrographs as well as the XRD results and Raman measurements[6] indicated that carbon inclusions in the sample were not attacked. Furthermore, the standard potentials indicated that the oxidation of carbon could take place only at much higher applied voltage in comparison to the SiC corrosion (Eqs. (2)–(9)). These observations indicate that the dissolution of the SiC can be described by Eqs. (3) and (7), reproduced here

$$SiC(s) + 2H_2O(l) \rightarrow SiO_2(s) + C + 4H^+(aq) + 4e^-$$

$$E^0 = -1.07\,V$$

and

$$SiC(s) + 6OH^-(aq) \rightarrow {SiO_3}^{2-}(aq) + C + 3H_2O(l) + 4e^-$$

$$E^0 = -1.87\,V$$

This is in agreement with the very low influence of CO_2 (Fig. 2d) or ${CO_3}^{2-}$[6,19] in the solution on the current density and open circuit potential.

The corrosion current densities of the SSiC materials observed here in acids are higher than those observed by Cook et al. In 1 M HCl in our experiments, values of 46 μA/cm^2 were observed, whereas Cook et al. observed values of 7 μA/cm^2. Our experiments with different holding times indicated that the current density could slow down by several orders of magnitude (see Fig. 2a), so the differences are probably connected with differences in the oxide layer thickness due to different holding times (preparation methods). Despite the lower stability of SiC in NaOH in comparison to acids, the initial corrosion current

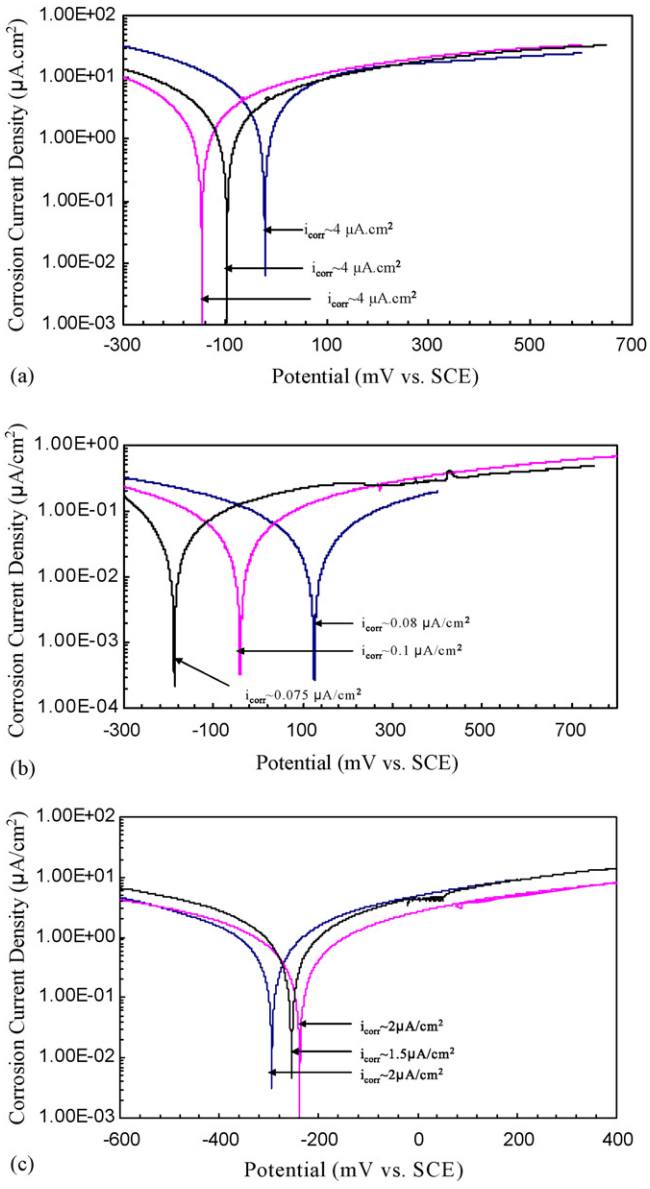

Fig. 4. Polarisation scans of the LPSSiC materials in different environments. (a) LPSSiC-1 in 1 M HNO_3, (b) LPSSiC-2 in 1 M HNO_3 and (c) LPSSiC-1 in 1 M NaOH.

densities measured for both conditions were similar. The different long term stabilities arise from the fast formation of SiO_2 layers in HCl and HNO_3 resulting in a strong reduction of the corrosion current density in acids.

As mentioned before, the corrosion current density of the LPS SiC materials was much lower than for the SSiC materials and was also different for the two LPS SiC materials investigated. The dissolution of the grain boundary regions in the LPS SiC materials could not contribute directly to the corrosion current since the said dissolution did not involve an exchange of electrons having been a simple hydrolysis reaction. The reduced corrosion current correlated neither with the resistivities of the materials nor with the volume content of the SiC in the material. It is possible that the doping of the SiC grains by Al and O changed the electrochemical reactions by which the grains

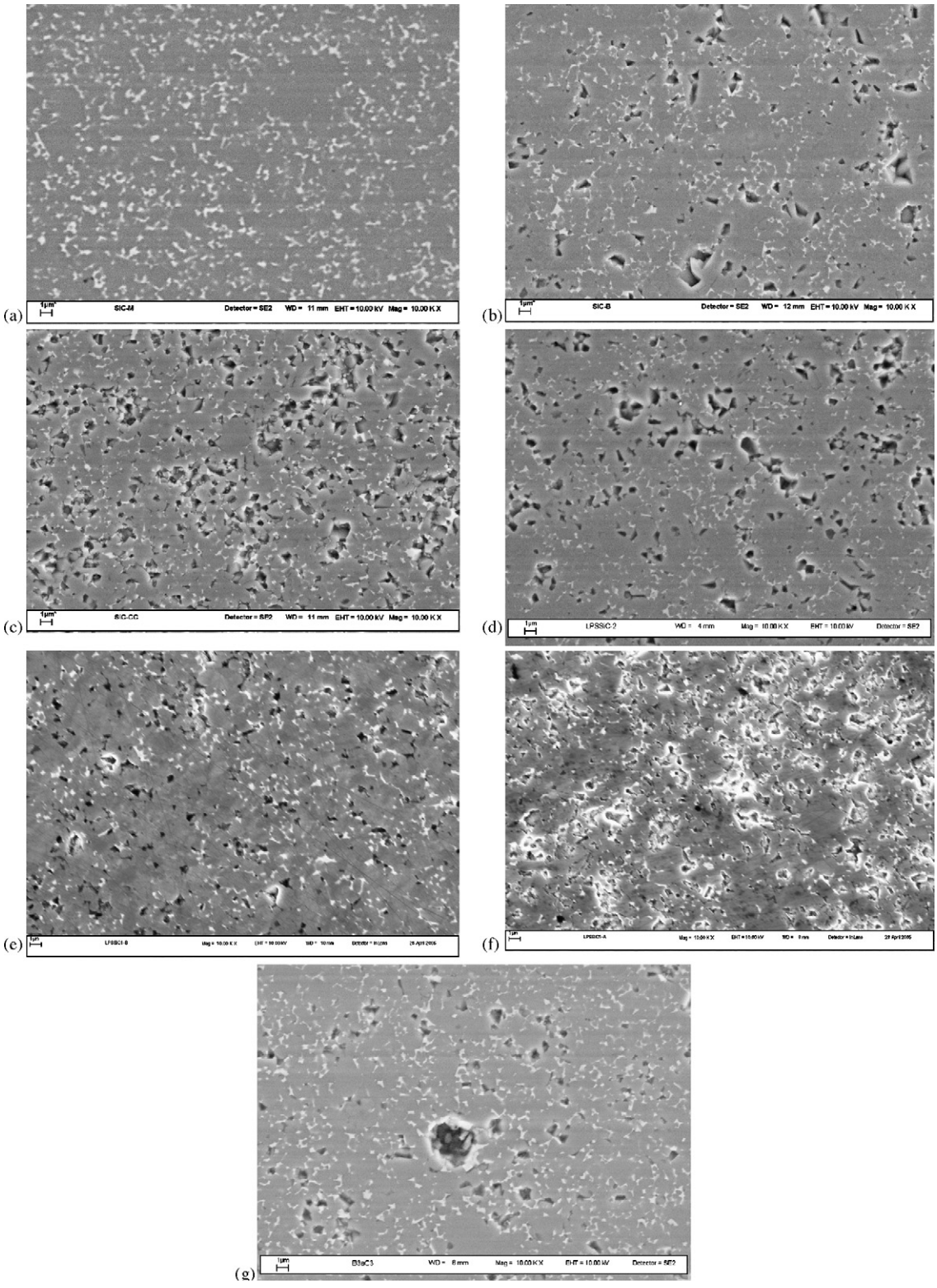

Fig. 5. SEM (secondary) micrographs of LPSSiC-1(a, c, e, f and g) and LPSSiC 2 (b and d) before and after corrosion. (a and b) LPSSiC-1 and LPSSiC-2 before corrosion, (c and d) LPSSiC-1 and LPSSiC-2 after full scan in 1 M HNO_3, (e) LPSSiC-1 after immersion in 1 M HCl. at +300 mV for 30 min, (f) LPSSiC-1 after immersion (without applying potential) for 30 min and (g) LPSSiC-1 after full polarisation scan in 1 M NaOH.

dissolve. Or that the presence of Y^{3+} and Al^{3+} ions changed the formation characteristics of any passivating surface layer.

The non-reproducibility of the E_{corr} of the LPS SiC materials observed here could have been caused by the chemical composition not being homogeneous throughout the test specimens as has been observed for stainless steels.[8] It has already been observed that Al, O and Y can dissolve in SiC grains influencing strongly the electrical behaviour of LPS SiC materials.[13–15]

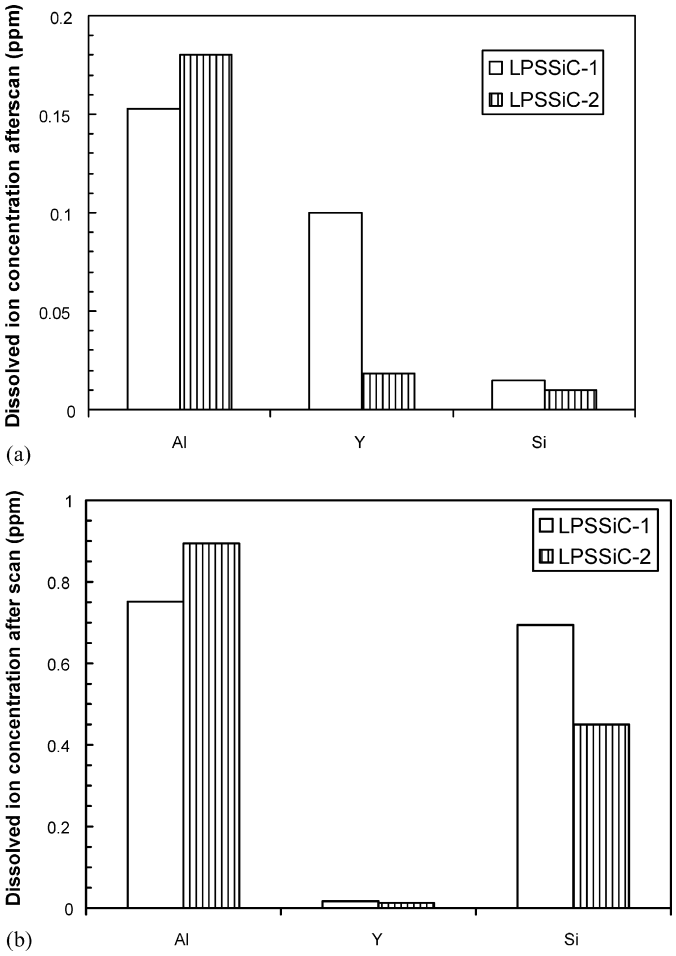

Fig. 6. Comparison of dissolved ion concentration of Si, Al and Y after full polarisation scans in (a) 1 M HCl and (b) 1 M NaOH.

The oxide additives seemed to affect also the current densities at higher applied potentials. For example comparing the current density at high potentials, for instance at +200 mV in 1 M HCl, the current density decreased by an order of magnitude (from 100 $\mu A/cm^2$ for SSiC to about 10 $\mu A/cm^2$ for LPS SiC materials) (Table 2).

The grain boundary regions of the LPS SiC materials were attacked in acids and bases much faster than the SiC-grains independent of the application of a potential (Fig. 5). The SEM figures (Fig. 5) showed that the dissolution of the grain boundary phase was not homogenous. This was caused by the different crystalline grain boundary phases (Table 1). Fig. 5 also showed that the dissolution in acidic and basic environment was slightly different. This observation was confirmed by ICP-OES analysis of the solutions after the corrosion tests (Fig. 6) which analysis indicated that compared to Si and Al, the yttrium concentration for both the LPS SiC materials were much lower in NaOH than in HCl. The much lower concentration of Y than Si and Al in NaOH could be associated with the formation of $Y(OH)_3$ which precipitates on the surface, inhibiting further dissolution of the grain boundary regions. Hence the less intense attack of the grain boundary phase observed in NaOH than in the acidic environments. The Al concentration was high in both NaOH and HCl because aluminium dissolves in strong alkaline environments forming $[Al(OH_6)]^{3-}$ or AlO_2^- ions. The silicon ion concentration in NaOH was higher than in HCl (Fig. 6), confirming the overall assumption[1–3,6] that in HCl a protective SiO_2 layer is formed on the SiC surface. Both LPS SiC materials showed similar amounts of dissolved Al ions in each of the electrolytes even though they had different amounts of alumina.

5. Conclusion

The corrosion of SSiC and LPS SiC ceramics has been investigated using electrochemical techniques in conjunction with microstructural examinations.

The corrosion of SSiC investigated here could be described by electrochemical methods. The electrochemical corrosion reaction of SiC was established to be the formation of C and SiO_2 protective layers in HCl and HNO_3 and carbon and soluble silicate ions in NaOH environment. The SiO_2 layer formed in HCl and HNO_3 caused a strong reduction of the corrosion current densities and a shift of the open circuit potential to more positive values. The carbon inclusions in SSiC did not dissolve in both acidic and alkaline environments under the test conditions used in this study.

The investigation of the LPS SiC materials, which contain yttria aluminium oxide grain boundary phase, indicates that the corrosion of these materials cannot be described fully by electrochemical methods because of the preferential dissolution of the grain boundary, which is a simple hydrolysis reaction that does not cause a corrosion current. The electrochemical corrosion in the LPS SiC materials was due to the dissolution of SiC. The corrosion current densities of the LPS SiC materials were more than an order of magnitude lower than those observed for SSiC. The reason for this behaviour is not completely clear and needs further investigation.

Acknowledgement

This work was partially supported by DAAD under an ANSTI fellowship award.

References

1. Schwetz, K.A., Silicon carbide based hard materials. In *Handbook of ceramic hard materials*, *Vol 2*, ed. Ralf Riedel, 2000, pp. 683–748.
2. Cook, G. S., Little, J. A. and King, J. E., Corrosion of silicon carbide ceramics using conventional and electrochemical methods. *Br Corros J*, 1994, **29**(3), 183–185.
3. Herrmann, M., Schilm, J., Michael, G. and Adler, J., Corrosion behaviour of different technical ceramics in acids, basic solutions and under hydrothermal conditions, in cfi/Ber. *DKG*, 2003, **80**(4), E27–E34.
4. Schwetz, A. and Hassler, J., Stability of high technology ceramics against liquid corrosion, cfi/Berichte. *DKG*, 2002, **79**(11), D14–D19.
5. Divakar, R., Seshadri, S. G. and Srinivasan, M., Electrochemical techniques for corrosion rate determination in ceramics. *J Am Ceram Soc*, 1989, **72**(5), 780–784.
6. Andrews, A., Electrochemical corrosion measurement of sintered silicon carbide and liquid phase sintered silicon carbide ceramics. MSc dissertation. University of the Witwatersrand, South Africa, 2005.
7. Meschke, F., Electrically driven cold water corrosion of SiC, in cfi/Ber. *DKG*, 2004, **81**(8), E19.

8. Jones, D. A., *Principles and prevention of corrosion* (*2nd ed*). Prentice-Hall, Inc., 1996.
9. Antelman, M. S., *The encyclopedia of chemical electrode potentials*. Plenum, New York, 1982, pp. 101, 183.
10. Bard, A. J., Parsons, R. and Jordan, J., Standard potentials in aqueous solutions, monographs. In *Electroanalytical chemistry and electrochemistry*, ed. A. J. Bard. Marcel Dekker, New York, 1985, pp. 189–206 [pp. 566–580, 587–629].
11. Pourbaix, M., Muylder, J. V., Besson, J. and Kunz, W., *Atlas of electrochemical equilibria in aqueous solution*. NACE, Houston. TX, 1958, pp. 449–463.
12. Scientific Group Thermodata Europe, Pure Substance Database, 2001.
13. Kleebe, H.-J. and Siegelin, F., *Z Metallkd*, 2003, **94**(3), 211–217.
14. Ihle, J., Martin, H.-P., Herrmann, M., Obenaus, P., Adler, J., Hermel, W. and Michaelis, A., The influence of porosity on the electrical properties of liquid phase sintered silicon carbide. *Int J of Mater Res*, 2006, **97**(5), 649–656.
15. Can, A., Herrmann, M., McLachlan, D. S., Sigalas, J. and Adler, J., Densification of liquid phase sintered silicon carbide. *J Eur Ceram Soc*, 2006, **26**, 1707–1713.
16. Rixecker, G., Wiedmann, I., Rosinus, A. and Aldinger, F., *J Eur Ceram Soc*, 2001, **21**, 1013.
17. Making potentiostatic and potentiodynamic anodic polarisation measurements, ASTM G5-94, Annual Books of ASTM Standards, 2000, *Vol 03.02*, pp. 57–67.
18. Conventions Applicable to Electrochemical Measurements in Corrosion Testing, ASTM G3-89, Annual Books of ASTM Standards, 2000, *Vol 03.02*, pp. 38–42.
19. Andrews, A., Herrmann, M. and Sephton, M., Electrochemical corrosion testing of solid state sintered silicon carbide in acidic and alkaline environments. *J South African Inst Mining Metall*, 2006, **106**, 269–276.